Magnetohydrodynamic Flow of Liquid-Metal in Circular Pipes for Externally Heated and Non-Heated Cases

A. Altintas[†] and I. Ozkol

Aeronautics & Astronautics Department, Istanbul Technical University, Istanbul, 34469, Turkey

†*Corresponding Author Email: altintas@itu.edu.tr*

ABSTRACT

The Computational Fluid Dynamics (CFD) study of external magnetic field effect on the steady, laminar, incompressible flow of an electrically conducting liquid-metal fluid in a pipe has been performed. The MHD Module of ANSYS Fluent commercial programme has been used to compute the flow and temperature fields. $Na^{22}K^{78}$ (sodium potassium) alloy has been used as operating fluid, which is liquid in room temperature. The simulations are performed for two different cases, first a non-heated pipe flow and secondly an externally heated pipe flow. For both cases, three different magnitude uniform external magnetic field, $\mathbf{B}_0$, applied (which are $\mathbf{B}_0 = 0.5$ T, 1.0 T and 1.25 T, T represents Tesla). The results are compared for the MHD effect on the flow variables in two cases separately, but also compared for heated and non-heated cases in order to analyze the temperature effect on MHD flows, as well. It is observed that heating is reducing the magnetic effect on the flow field. While in non-heated cases it is observed that very well-known slowing down effect of MHD on fluid flow, in heated case the velocity field shows a tendency to behave as if it were MHD is not applied. Towards the end of the physical length the heating seems dominating the MHD effect. It is shown that in heated case temperature differences and entropy differences are in tendency to behave as if it were MHD is not applied.

Keywords: MHD flow; Heat flux; Temperature; Pipe; Entropy; Liquid-metal.

NOMENCLATURE

B	total magnetic field vector	q	electric charge density
B_0	external applied magnetic field vector	q"	heat flux vector
b	induced magnetic field vector	Re_m	magnetic Reynolds number
D	induction field vector for electric field	S	Siemens
d	the pipe diameter	T	temperature
E	the electric field vector	T	tesla
H	induction field vector for magnetic field	T_{env}	environment temperature of the pipe
Hm^{-1}	henries per meter	u	velocity vector
h	heat transfer coefficient	u	velocity in axial direction
J	the electric current density vector	U_{in}	the pipe inlet velocity
k	thermal conductivity		
l	length of the pipe	ε	electric permittivity
MHD	magnetohydrodynamics	μ	dynamic viscosity
$Na^{22}K^{78}$	sodium potassium alloy	μ_0	magnetic permeability
Nu	Nusselt number	ν	kinematic viscosity
p	pressure	σ	electrical conductivity

1. INTRODUCTION

The control of electrically conducting fluids is getting more and more importance in recent years. Magnetohydrodynamics (MHD) flow control method is one of the commonly used. After Hartmann (1937) investigations on the MHD flow of a viscous, incompressible, electrically conducting fluid now the MHD flow finds a wider range area of study (Grigoriadis *et al.* 2009; Jing *et al.* 2013; Gedik *et al.* 2012; Kumar *et al.* 2013). The studies on MHD are becoming much important since these type flow fields are commonly encountered in many engineering fields such as at nuclear reactors as a coolant fluid (Sheng 1990). Also recent developments such as Lorentz Force Velocimetry (LFV) which uses reacting force of the fluid to the Lorentz force (Thess *et al.* 2006; Jian and Karcher 2012) makes the MHD flow studies more popular.

Self-cooled liquid metal blankets in fusion reactor systems could be given as one of the mostly used application of liquid metal flows. Due to high heat transfer coefficients, the liquid metals show high heat transfer performances. This characteristic makes this kind of liquids a best option as a working fluid in fusion reactor systems (Serizawa *et al*. 1990). However the liquid metals also has high electrical conductivity which causing large magnetic pressure drop (Cuevas *et al*. 1997; Ying and Gaizer 1995). One of the way to reduce the MHD pressure drop is to apply an electrically insulating coating on the duct walls (Malang and Tillack 1995).

In this study the effect of uniform magnetic field on the velocity field of an electrically conducting liquid metal flow in a circular pipe has been investigated. Also externally applied uniform heat flux together with magnetic field is applied to investigate the interactions of heat and MHD effects. $Na^{22}K^{78}$ alloy has been used as liquid metal. The eutectic mixture $Na^{22}K^{78}$ consists of 78% potassium and 22% sodium, is liquid at a temperature higher than -10ºC, and has a density of 866 kg/m^3 at 21ºC. The kinematic viscosity, ν, electrical conductivity, σ, and magnetic permeability, μ_0, are 9.8498×10^{-4} kg/ms, 2.457×10^{-6} S/m, $4\pi \times 10^7$ H/m, respectively. The paper arranged as follows. First, the problem description and methods are presented by providing a brief description of the magnetic induction method which is the method applied by the MHD module of ANSYS Fluent. In the following sections the paper divided in two parts, in the first part non-heated pipe flow with MHD applied case results are given. In the second part externally heated pipe flow together with the MHD effects are given, then the results are compared with the non-heated cases. In the final section some concluding remarks are given.

1.1 Problem Description

The study has been divided into two parts; in first part it is considered the flow of a steady, laminar, viscous, conducting liquid-metal in circular pipe under the influence of a uniform transverse magnetic field with constant pressure gradient which can be seen schematically in Fig. 1. The pipe length is choosen as $l = 300$ *mm* and diameter choosen as $d = 10$ *mm*. The uniform magnetic field applied perpendicular to the flow direction. In second part, it has been implemented additional constant heat flux, q", as a difference from the non-heated case. The pipe inlet velocity is $U_{in} = 0.05$ *m/sn* in order to achieve a laminar flow in pipe with given fluid and pipe properties. T_{env} represents the temperature of the environment.

The magnetic Reynolds numbers, $Re_m = \mu_0 \sigma \nu Re$ is in the order of 10^{-7}. In the case of $Re_m \ll 1$ induced magnetic field, b, is much smaller compare to applied magnetic field, B_0. This means the induced magnetic field can be negligible in the total magnetic field, B. The governing equations of an incompressible electrically conducting liquid-metal fluid in circular pipes can be given with Navier-Stokes equations;
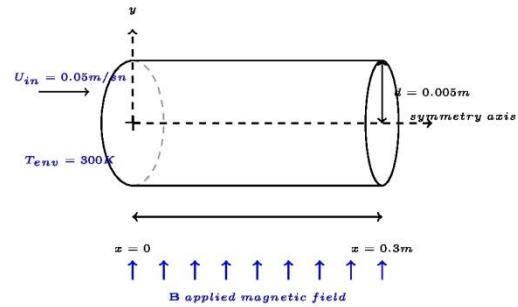

Fig. 1. Illustration of the cylinder pipe.

$$\frac{\partial u}{\partial t} + u \cdot \nabla u = -\frac{1}{\rho}\nabla p + \nu \nabla^2 u + \frac{1}{\rho}(J \times B), \qquad (1)$$

$$\nabla u = 0. \qquad (2)$$

Electromagnetic fields are described by Maxwell's equations:

$$\nabla \cdot B = 0, \qquad (3)$$

$$\nabla \times E = -\frac{\partial B}{\partial t} \qquad (4)$$

$$\nabla \cdot D = q, \qquad (5)$$

$$\nabla \times H = J + \frac{\partial D}{\partial t}, \qquad (6)$$

The induction fields H and D are defined as,

$$H = \frac{1}{\mu} B, \tag{7}$$

$$D = \varepsilon E, \tag{8}$$

The problem given has been solved with using ANSYS Fluent MHD Module. In non MHD case applied magnetic field has been solved by exploit symmetry of the geometry (see Fig. 1). The magnetic induction method has been choosen in MHD module, which can be found in following section.

1.2 Magnetic Induction Method

In general Ohm's Law that defines the current density is given by;

$$J = \sigma E \tag{9}$$

for fluid velocity field u in a magnetic field B,

$$J = \sigma (E + u \times B) \tag{10}$$

From Eq. 4;

$$\frac{\partial B}{\partial t} = -\nabla \times E, \tag{11}$$

From Eq. 10;

$$E = -\frac{J}{\sigma} - u \times B, \tag{12}$$

Take the curl;

$$\nabla \times E = \nabla \times \left(\frac{J}{\sigma} - u \times B \right), \tag{13}$$

Inserting Eq. 13 into Eq. 11 we get,

$$\frac{\partial B}{\partial t} = -\nabla \times \left(\frac{J}{\sigma} - u \times B \right), \tag{14}$$

$$\frac{\partial B}{\partial t} = -\nabla \times \left(\frac{J}{\sigma} \right) + \nabla \times (u \times B), \tag{15}$$

if the displacement current neglected customarily, we rewrite Eq. 6 as,

$$\nabla \times H = J, \tag{16}$$

with using Eq. 7,

$$\frac{1}{\mu} (\nabla \times B) = J, \tag{17}$$

if we substitute Eq. 17 into Eq. 15 we get,

$$\frac{\partial B}{\partial t} = -\nabla \times \left(\frac{1}{\mu\sigma} (\nabla \times B) \right) + \nabla \times (u \times B), \tag{18}$$

could be written as;

$$\frac{\partial B}{\partial t} = -\frac{1}{\mu\sigma} \nabla \times (\nabla \times B) + \nabla \times (u \times B) \tag{19}$$

Here if we use the very well-known property; $a \times (b \times c) = b(a \cdot c) - c(a \cdot b)$ rewrite the Eq. 19,

$$\frac{\partial B}{\partial t} = -\frac{1}{\mu\sigma} (\nabla(\nabla \cdot B) - B(\nabla \cdot \nabla))$$
$$+ u(\nabla \cdot B) - B(\nabla \cdot u), \tag{20}$$

with using Eq. 3,

$$\frac{\partial B}{\partial t} = \frac{1}{\mu\sigma} \nabla^2 B + u(\nabla \cdot B) - B(\nabla \cdot u) \tag{21}$$

arranging Eq. 21 we get,

$$\frac{\partial B}{\partial t} + B(\nabla \cdot u) = \frac{1}{\mu\sigma} \nabla^2 B + u(\nabla \cdot B). \tag{22}$$

Eq. 22 is the induction equation derived from Ohm's law and Maxwell's equations. By solving Eq. 22 it is possible to obtain B, and using the B it is possible to obtain the J (see Eq. 17).

1.3 Solution Method

A laminar viscous model is used in ANSYS Fluent. Electrically insulating wall boundary conditions have been choosen for MHD boundary conditions. No-slip boundary conditions are also applied at walls which means axial velocity which is along the centerline of the pipe, u, equal to wall velocity;

$$u_{wall} = 0. \tag{23}$$

Velocity boundary conditions are implemented at inlet, this is;

$$U_{in} = 0.05 \, m / sn, \tag{24}$$

for non-heated cases. The below are the boundary conditions for heat flux applied cases,

$$U_{in} = 0.05 \, m / sn, T_{in} = 300 \, K. \tag{25}$$

Pressure boundary conditions are implemented in the outlet which is;

$$P_{x=l} = P_{atm} \tag{26}$$

Pressure based solver has been used. SIMPLE scheme is used for pressure-velocity coupling, second order upwind discretization approach used for all pressure, momentum, energy and magnetic field equations. In all the simulations before applying MHD effect, flow field variables are allowed to reach a fully developed state.

For the externally heated pipe case, all the above developed solution approaches methods together with an externally applied constant heat flux, q", and inlet temperature, T_{in} are applied.

2. RESULTS AND DISCUSSION

2.1 Part I: MHD in non-heated Pipe Flow

In Fig. 2 simulation results for all four different magnitude of B_0 magnitudes for axial velocity are given. However for B = 0T and B = 0.5T cases results are seems similar, there is a slow down in fluid flow which is more clear for cases B = 1T and B = 1.25T.

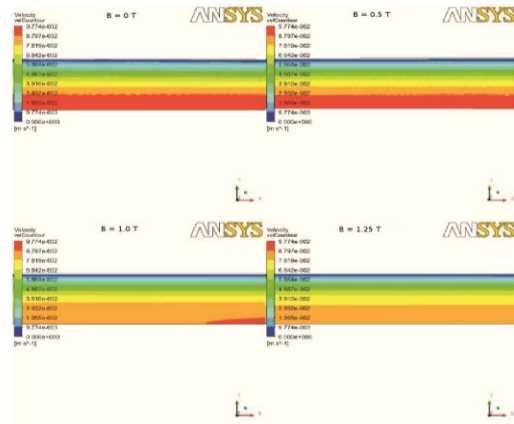**Fig. 2. The velocity contours from the upper symmetric part of the cylinder pipe.**

Figure 3 represents the axial velocity in radial direction for the upper half of the pipe from the four different locations along the pipe. These locations are $x = 50$ *mm*, 150 *mm*, 250 *mm* and 298 *mm*, respectively. While $d = 0$ represents the symmetry axis, x, $d = 0.005$ represents the periphery of the cylinder as measured meter.

It is note that the pipe flow reacts a fully developed state about the location $x = 250$ *mm*. In non-magnetic force applied case (B = 0T), the velocity of the pipe is approximately 0.1 *m/sn* at the just about the pipe outlet, though in magnetic force applied case the velocity values are getting lower depending on the strength of the applied external magnetic field. This retardation of the fluid flow under the magnetic field effect has been observed by many authors (Cuevas *et al.* 1997; Raja *et al.* 2012; Seth and Singh 2013). Same reduction is observed for four different locations.

Skin friction coefficient, *Cf(x)=τw/0.5ρU∞,* ($U_\infty = U_{in}$ in this case) is an important parameter give a sense about the behavior of field variables near the wall. It has observed higher skin friction coefficient in force applied cases compare to no-force applied cases (Fig. 4). This could be explained as; in MHD applied cases it has been observed more flat velocity profiles, since in order to keep uniform mass flow the axial velocity near the wall is getting increase in magnitude (Fig. 3). This increase causing a higher velocity gradients near the wall which also causes higher shear stress hence
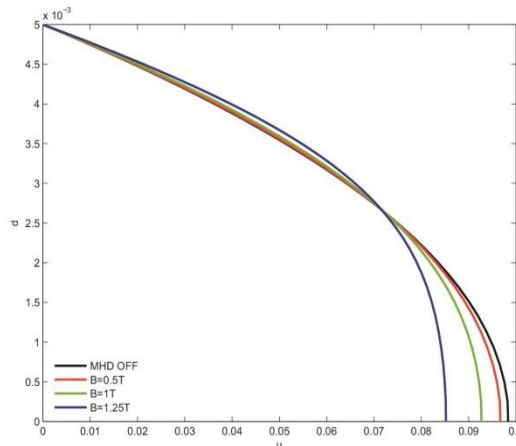
higher skin friction coefficient near wall (Fig. 4). The similar results found by Malekzadeh *et al.* (2011).
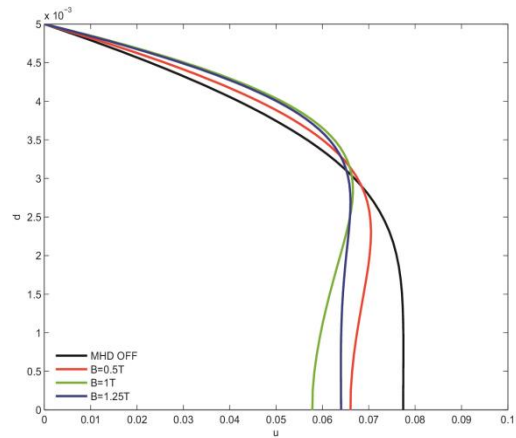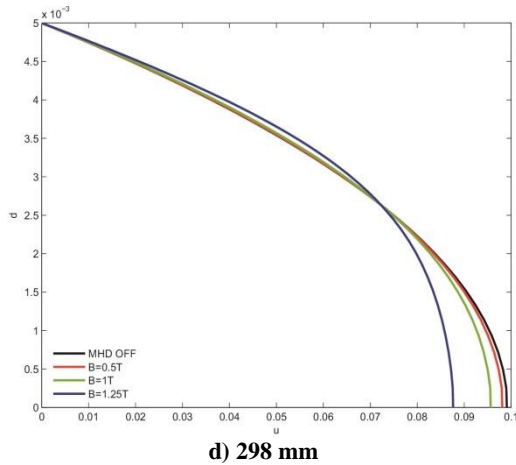

a) x=50 mm
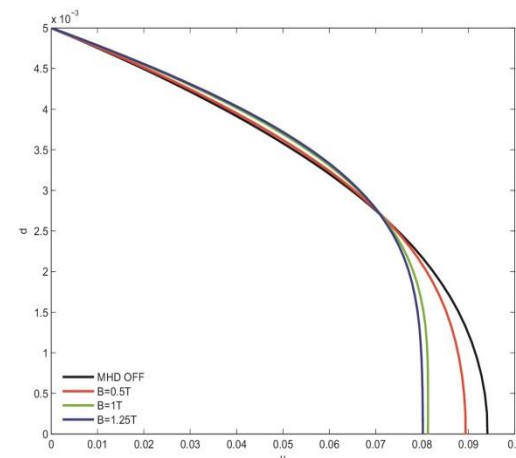
b) x=150 mm

c) x=250 mm

d) 298 mm

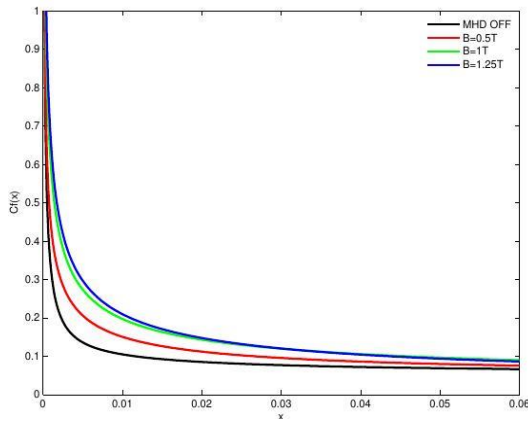**Fig. 3. Axial velocity from the four different locations.**

Fig. 4. Skin friction coefficient, *Cf(x)*, from the wall of cylinder pipe.
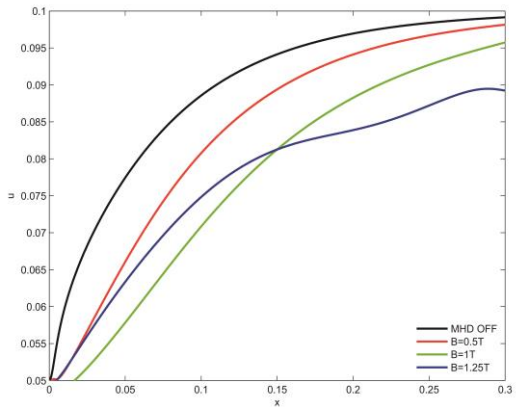

Fig. 5. Axial velocity on symmetry axis for non-heated pipe cases.

Figure 5 represents the streamwise velocity change in streamwise direction at symmetry axis of the circular pipe. Clearly the centre of the flow field is effected strongly by the magnetohydrodynamic forces. Interestingly while for B = 0 T, 0.5 T and 1T cases

there is an approximately linear change at velocity, for B = 1.25T case there is a sudden increase at rate of change of velocity decrease after the half length of the channel.

2.2 Part II: MHD in Heated Pipe Flow

In this part of the study it is implemented constant heat flux, q''=79,000*W/m²*, applied externally as shown in Fig. 6, as a difference from the problem studied in the previous section. MHD effect and temperature interaction has been investigated and the results are compared to non-heated cases.
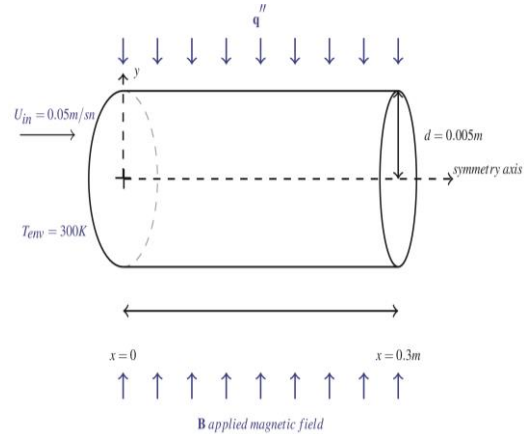

Fig. 6. Illustration of cylinder pipe.

In Fig. 7 it is observed that the skin friction coefficient for heated pipe flow, has similar tendency with the non-heated case.

However if one takes a close look at Fig. 8, which represents the axial velocity along the pipe on the symmetry axis, it is obviously notices that there exist a greater gradient in mechanism slowing the flow compare to heated case (Fig. 5). The difference between heated and non-heated cases getting higher for higher applied magnetic fields, B_0. Considering all flow field variables under the application of various magnetic field strength it has been observed that before the flow field fully developed (*x* < 250 *mm*) magnetic strength dominates field variables, after the fully developed section (*x* ≥ 250 *mm*) this domination is reduced dramatically.

It is also observed similar trend in Nusselt number, Nu = *hd/k*, which represents the rate of heat transfer in upper wall of pipe given in Fig. 9 which results are parallel with the study of Malekzadeh *et al.* (2011); Li *et al.* (2005).

In Fig. 10 the temperature gradients, *dT/dy* are shown for four different locations. If these plots are analysed it is noticed that there exist a diminishing temperature gradient difference along the axial line of the pipe. It is also plotted the axial velocities for the same locations in Fig. 11. It is similar trend is observed in axial velocity along the pipe. It is note that the pipe flow here reachs a fully developed state starting from

$x = 250$ *mm* point of the pipe. Before that point MHD seems effective however not effective as non-heated cases (Figs. 11(a), 11(b) and Figs. 3(a), 3(b)). However in non-heated case, starting from fully developed location of the pipe, the very well-known results of MHD is observed as expected. These effects show themselves as a slowdown process on the flow field. The temperature gradient difference seems to be diminished as MHD effect along the pipe axis in non-heated case (Figs. 11(c), 11(d) and Figs. 3(c), 3(d)). These results suggest that MHD affects temperature field and vice versa.

Before the fully developed section increasing magnetic field strength has a decreasing effect on the entropy generation. However after passing fully developed section, increasing magnetic field strength has no effect in the entropy generation (Fig. 12).
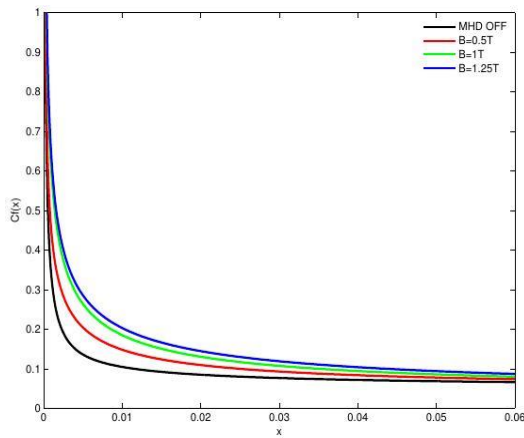

Fig. 9. The Nusselt number, Nu, which defines the rate of heat transfer, from the upper wall of the pipe.
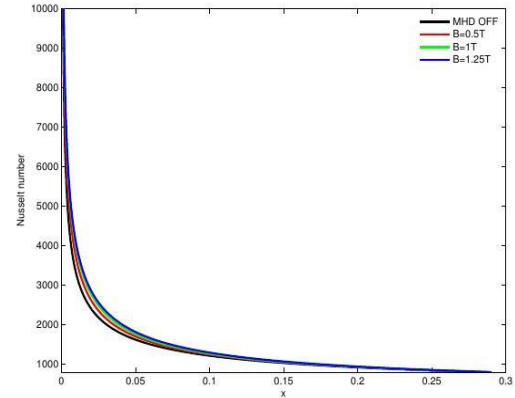

Fig. 7. Skin friction coefficient, *Cf (x),* for heated pipe cases.

(a) $x = 50$ *mm.*   (b) $x = 150$ *mm.*

(c) $x = 250$ *mm.*   (d) $x = 298$ *mm.*
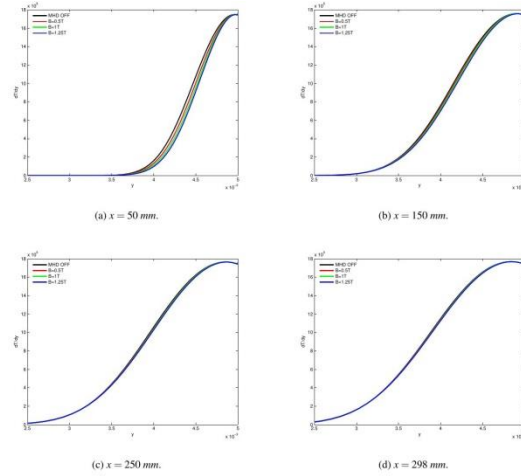
Fig. 10. The temperature gradient from the four different locations.

Fig. 8. Axial velocity on symmetry axis for heated pipe cases.

(a) $x = 50$ *mm.*   (b) $x = 150$ *mm.*

(c) $x = 250$ *mm.*   (d) $x = 298$ *mm.*
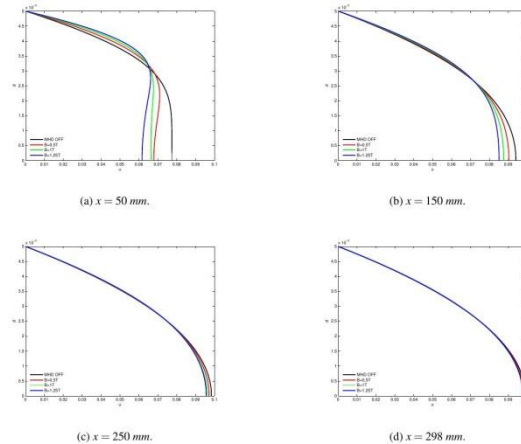
Fig. 11. Streamwise velocity for heated cases from four different locations.

(a) $x = 50$ *mm.*

(b) $x = 150$ *mm.*

(c) $x = 250$ *mm.*

(d) $x = 298$ *mm.*

Fig. 12. Entropy from the four different locations.
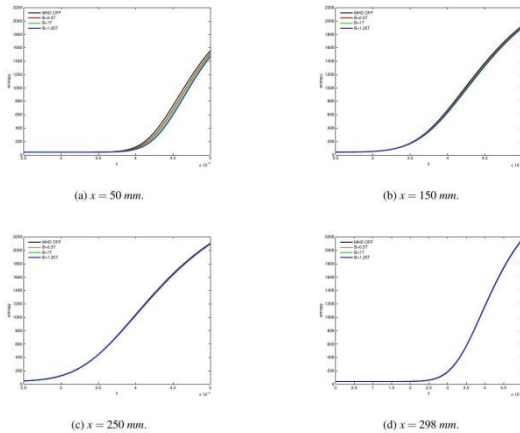
3. CONCLUSIONS

In this study two different MHD pipe flow cases have been investigated, first non-heated MHD pipe flow, secondly the heated case. The results are discussed with comparing the flow and temperature fields related to fully developed and non-fully developed sections are discussed.

It is obtained very well known retarded flow in former case (Fig. 3), but in latter case it is observed that MHD affects temperature and vice versa. It is noted that the velocity field reachs its fully developed case at $x = 250$ *mm*. However there exist a MHD effect in heated cases, this effect lower than non-heated cases for the sections below $x = 250$ *mm*, it seems temperature altered the MHD effect along the axial direction of the pipe. In the area close to the outlet of the pipe, the temperature differences between non MHD applied case and MHD applied cases are diminishing which is a result of magnetic field and temperature field interactions.

The temperature gradient, *dT/dy* and entropy, are depicted for heated cases, as well (Figs. 10, 12). Before the fully developed section, increasing magnetic field strength has a decreasing effect on the entropy generation. However after passing fully developed section, increasing magnetic field strength has no effect in the entropy generation (Fig. 12). Similar results are observed for the temperature gradient, while the area below fully developed location, increasing magnetic field strength has an increase effect on the temperature gradient, these differences are slowly overcome toward the pipe outlet (Fig. 10).

REFERENCES

Cuevas, S., B. Picologlou, J. S. Walker, and G. Talmage (1997). Liquid-metal MHD flow in rectangular ducts with thin conducting or insulating walls: laminar and turbulent solutions. *Int, J. Engng Sci.* 35(5), 485-503.

Gedik, E., H. Kurt, Z. Recebli, and C. Balan (2012). Two-dimensional CFD simulation of magnetorheological fluid between two fixed parallel plates applied external magnetic fields. *Computers & Fluids* 63, 128-134.

Grigoriadis, D. G. E., S. C. Kassinos, and E. V. Votyakoy (2009). Immersed boundary method for the MHD flows of liquid metals. *J. Compt. Phys.* 228(3), 903-920.

Hartmann, J. (1937). Theory of the laminar flow of an electrically conductive liquid in a homogeneous magnetic field. *Mathematisk-fysiske Meddelelser* 15(6).

Jian, D. and C. Karcher (2012). Electromagnetic flow measurements in liquid metals using time-of-flight Lorentz force velocimetry. *Meas. Sci. Technol.* 23(7).

Jing, Z., M. -J. Ni, and Z. -H. Wang (2013). Numerical study of MHD natural convection of liquid metal with wall effects. *Numerical Heat Transfer* 6(4), 563-569.

Kumar, H. (2012). Radiative heat transfer with MHD free convection flow over a stretching porous sheet in presence of heat source subjected to power law heat flux. *Journal of Applied Fluid Mechanic,* 6(4), 563-569.

Li, F. C., T. Kunugi, and A. Serizawa (2005). MHD effect on flow structures and heat transfer characteristics of liquid metal-gas annular flow in a vertical pipe. *Int. J. Heat Mass Trans.* 48(12), 2571-2581.

Malang, S. and M. S. Tillack (Eds.) (1995). Development of self-cooled liquid metal blankets. *FZK report, FZKA 5581.*

Malekzadeh, A., A. Heydarinasab, and D. Bahram (2011). Magnetic field effect on fluid flow characteristics in a pipe for laminar flow. *J. Mech. Sci. and Tech.* 25(2), 333-339.

Raja, T., S. Karthikeyan, and B. Senthilnathan (2013). A magneto-convection over a semi-infinite porous plate with heat generation. *Journal of Applied Fluid Mechanics* 6(4), 589-595.

Rao, J. A., R. S. Raju, and S. Sivaiah (2012). Finite element solution of heat and mass transfer in MHD flow of a viscous fluid past a vertical plate under oscillatory suction velocity. *Journal of Applied Fluid Mechanics* 5(3), 1-10.

Serizawa, A., T. Ida, O. Takahashi, and I. Michiyoshi (1990). MHD effect on NaK-Nitrogen two-phase flow and heat transfer in a vertical round tube.

Int, J. Multiphase Flow 16(5), 761-788.

Seth, G. S. and J. K. Singh (2013). Effects of hall current on unsteady MHD coquette flow of class-II in a rotating system. Journal of Applied Fluid Mechanics 6(4), 473-484

Sheng, R. (1990). The effect of magnetic field on two-phase liquid metal flow. *Acta Mechanica Sinica* 6(2), 128-132 .

Thess, A., E. V. Votyakov, and Y. Kolesnikov (2006). Lorentz force velocimetry. *Phys. Rev. Lett.* 96(April).

Ying, A. Y. and A. A. Gaizer (1995). The effects of imperfect insulator coatings on MHD and heat transfer in rectangular ducts. *Fusion Engineering and Design.* 27, 634-641.